



## Effect of Hot Rolling on the Mechanical and Corrosion Properties of AlTiB<sub>2</sub> Composites

<sup>1</sup>Amith Kumar S N, <sup>2</sup>Dr. T. N Raju

<sup>1</sup>Assistant professor, Department of Mechanical Engineering, Dr Ambedkar Institute of Technology, Visvesvaraya Technological University, Bangalore-560060, Karnataka, India..

<sup>2</sup>Associate professor & head, Department of Mechanical Engineering, Dr Ambedkar Institute of Technology, Visvesvaraya Technological University, Bangalore-560060, Karnataka, India..

**Abstract:** - Aluminium matrix composites reinforced with varying weight percentages (0,2,4,5,6,8 and 10%) of TiB<sub>2</sub> were fabricated using the stir casting process and the in-situ approach. The dispersion and existence of TiB<sub>2</sub> particles within the Al matrix were confirmed through SEM and EDAX analysis, showing reasonably good dispersion. Cold rolling of the composites led to grain elongation along the rolling direction, impacting grain distribution significantly, especially at extreme rolling temperatures. Hot rolled composites with 4%,6% and 8% TiB<sub>2</sub> exhibited higher Vickers micro hardness values compared to pure Al 2011. Additionally, cold rolled samples demonstrated higher micro hardness compared to hot rolled counterparts with the same TiB<sub>2</sub> content. The inclusion of TiB<sub>2</sub> in Al composites contributed to the formation of a protective layer, enhancing the material's strength. Wear rates decreased with increasing TiB<sub>2</sub> content, corresponding to higher hardness values and more uniform dispersion of the reinforced phase. Tensile and yield strengths of cold-rolled samples increased with TiB<sub>2</sub> content due to the presence of significant dislocation density. However, hot rolling resulted in decreased yield strength and % of elongation due to preceding heat treatments. Overall, the study highlights the influence of TiB<sub>2</sub> content and processing methods on the mechanical properties and microstructure of AlTiB<sub>2</sub> composites.

**Keywords:** In-situ, SEM, EDAX, Hot Rolling, Cold Rolling, AlTiB<sub>2</sub>.

### Introduction

For MMCs, Al is the most widely used matrix. Due to its high specific strength, stiffness, wear resistance, and superior dimensional stability, Al-MMCs are widely used in the aerospace, automotive, and other industries [1].

Al-based MMCs have recently been created using in-situ procedures, which may improve adhesion at the interface and, consequently, the mechanical properties. Numerous benefits come from these in-situ methods, including stronger particle matrix bonding, more uniform



dispersion within the matrix, thermodynamic stability, and surface contamination-free in-situ generated reinforcing phases [2]. Corrosion is the term used to describe the destructive attack of a metal by chemicals, the environment, or electrochemical processes on all metals and alloys [3].

Corrosion reactions are known as interfacial processes because they often take place on the metal surface. Because the corrosion process occurs at the metal medium phase boundary, it is a heterogeneous reaction in which the metal surface's structure and state play a major influence. It is necessary to carry the corrosive medium to the surface and extract the corrosion products. Consequently, it is also necessary to include material transport phenomena such as free convection and diffusion into nearby surface layers. A variety of metallurgical parameters, such as residual stress from cold work, impurity inclusions, crystallography, and grain size and shape and heterogeneity, can influence corrosion in an alloy.

Studies have been conducted on the effects of nitric acid ( $\text{HNO}_3$ ) on the corrosion of Al-Cu alloys with 1.330 at. % Cu [3]. They discovered that, in  $\text{HNO}_3$ , the corrosion rates of the Al-1.3 at. % Cu and Al-2.7 at. % Cu alloys were, respectively, about 5 and 10  $\text{nm min}^{-1}$ . With a local rate of  $\sim 13 \text{ nm s}^{-1}$ , the corrosion of an Al-30 at. % Cu alloy was less uniform. Meanwhile, in 1.0 M  $\text{Na}_2\text{SO}_4$  solution at 25 °C, [4] have investigated the pitting corrosion of  $\text{ClO}_4^-$  on pure Al, Al-2.5 wt.% Cu, and Al-7 wt.% Cu alloys. The three Al samples exhibit decreasing sensitivity to pitting corrosion in the following order: Al>Al-2.5 wt.% Cu>Al-7 wt.% Cu.

Potentiostatic experiments revealed that while the rate of pitting initiation decreases with increasing Cu content, it increases with increasing  $\text{ClO}_4^-$  ion concentration and applied step anodic potential. In  $\text{Na}_2\text{SO}_4$  solutions, the corrosion behaviour of pure aluminium, aluminium-6% Cu, and aluminium-6% Si alloys was investigated in the presence and absence of NaCl, NaBr, and NaI [5]. The order of increase in corrosion resistance is Al<Al-6%Cu<Al-6%Si. The most aggressive ion was the chloride ion. Their research aims to determine how Cu addition affects the mechanical characteristics and corrosion resistance of commercially pure aluminium.

Cu addition on the mechanical properties and corrosion resistance of commercially pure Al have been investigated [6]. They studied the influence of Cu addition to commercially pure aluminium on microstructure, microhardness, grain size, impact energy, flow stress at 0.2 strain, mechanical behaviour and corrosion resistance. Three different Al-Cu alloys of 3, 6 and 9 wt.% Cu content were prepared and experimentally tested both mechanically and chemically. The results show the addition of Cu resulted in a linear increase of the hardness, and substantial reduction in the grain size, slight reduction the impact energy, substantial increase in the flow stress at 0.2 strains, and improve in the mechanical properties. Potentiostatic experiments revealed that the samples' sensitivity to corrosion falls in the following order: Al>Al-3 wt.%



Cu>Al-9 wt.% Cu>Al-6 wt.% Cu. Three, six, and nine weight percent Cu alloys were found to corrode at rates of 0.29, 0.13, and 0.21 nm/s in HCl, respectively. The various attributes, such as impact energy, flow stress at 0.2 strain, mechanical qualities, and corrosion resistance, demonstrated that the composition of 6% Cu is ideal.

## Materials and Methods

The basic matrix is made of Aluminium 2011 Alloy. Production of Composites with AlTiB<sub>2</sub> to obtain 0%,2%, 4%,5% 6%,8%, and 10% of AlTiB<sub>2</sub> composites, a metal matrix utilizing the "in situ" stir casting procedure was created using aluminium alloy 2011 and two halide Salts (K<sub>2</sub>TiF<sub>6</sub> and KBF<sub>4</sub>) are employed as reinforcements. The furnace is filled with halide salts and aluminium alloys. After getting the mixture to a molten stage, the molten is poured into a mould box to create a plate. After then, the cast specimen is hot-rolled. The deformation is seen on the plate following hot rolling. To acquire the necessary dimension for testing, additional rolled specimens are put through a machining procedure. Tests for corrosion are carried out to assess anticorrosion qualities. An assessment of the mechanical properties of AlTiB<sub>2</sub> composites, including hardness, tensile strength, and wear parameters, is carried out. SEM and EDAX are used, respectively, to investigate the presence and dispersion of TiB<sub>2</sub> particles in the Al matrix.

## Hot Rolling and Machining Process

In this study the hot rolling process and machining of AlTiB<sub>2</sub> composites are discussed.

### Hot Rolling

In the hot rolling process, metal is heated above the temperature at which it recrystallizes, causing it to plastically deform during the working or rolling activity.

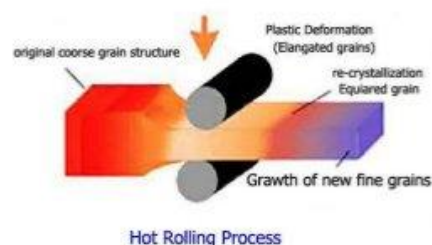


Fig 1. Schematic view of setup hot rolling

In this study, Cast Product were hot rolled at a constant strain rate of  $6 \times 10^{-3}/s$  and a rectangular specimen from cast products wire cut and heated for 1 hour at a temperature of 400 degree Celsius. The specimen was placed through hot rolling process with a



reduction of 10% in each pass, after the heating was completed an 50% reduction the hot rolled sheet were obtained. (Using 2-High rolling mill the Al cast specimen was hot rolled).

### Hot rolled specimen:

Fig 2 and Fig 3 shows specimen of Before and After Rolling process.

**Before Rolling**

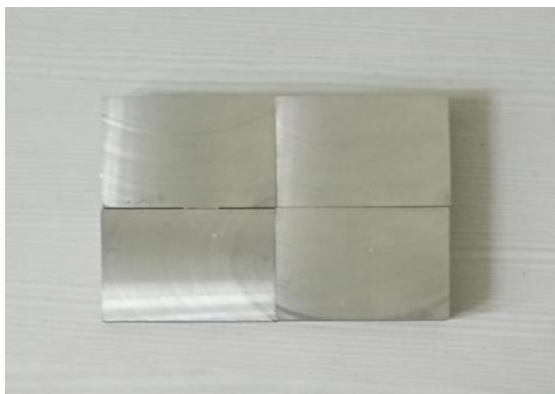


Fig: 2. Shows Specimens before Rolling  
after Rolling

**After Rolling**



Fig: 3. Shows Specimens

### Machining Process:

Any procedure where a cutting tool is used to remove tiny material chips from the workpiece—often referred to as the "work"—is called machining. The tool and the work must move relative to one another in order to complete the process. Most machining operations use a main motion called "cutting speed" and a secondary motion called "feed" to produce this relative motion. These actions, along with the geometry of the tool and its penetration into the work surface, result in the desired shape of the final work surface.

## STUDY OF MECHANICAL AND CORROSION PROPERTIES

### Hardness Test

Using the Vickers micro hardness tester, specimens of alloy and MMCs were subjected to micro hardness tests at a load of 100 grams and a dwell duration of 10 seconds. Each





specimen's hardness was measured three times at different locations, and the results were given.

The material being tested is much softer than the indenter, which is typically shaped like a ball, pyramid, or cone and is typically made of hardened steel, tungsten carbide, or diamond. Care should be used when comparing values obtained using different procedures because measured hardness is just relative and not absolute. ASTM E 383 standards were followed when conducting the tests.

### SEM Characterization:

Conventional polishing was used to prepare samples for scanning electron microscopes (SEMs). Samples were polished in a 0.3 m alumina slurry first, then in P220 Silicon Carbide emery paper. After polishing, samples were thoroughly cleaned with DI water and dried with a blast of air. The polishing procedure in Vibro-Meter was finished using a 0.04 m colloidal silica solution. Following final polishing, the samples were ultra-solicted in ethanol for ten minutes. Samples were maintained in a desiccator with a relative humidity of less than 10%.

The microstructure was revealed by mechanically polishing cut specimens under a scanning electron microscope. Using Keller's reagent, chemical etching was done to expose SEM.

### Tensile Test

The destructive test technique known as tensile testing provides information regarding the tensile strength, yield strength, and ductility of metallic materials. It evaluates the stretch or elongation that a plastic or composite specimen must experience in order to break. Tensile strength of AlTiB<sub>2</sub> composites was measured using UTM in accordance with ASTM E8 standard. The specimen dimensions for the tensile test are shown in Fig. 4.

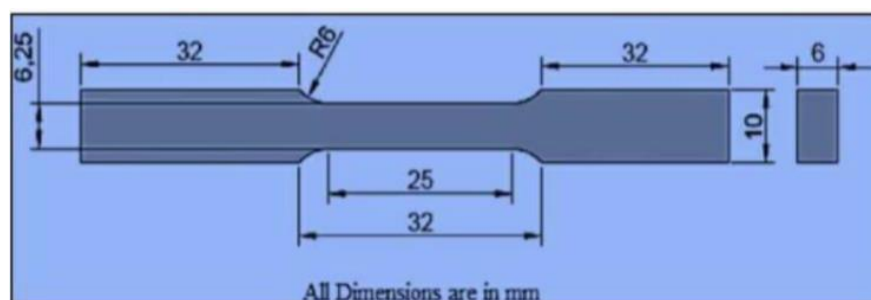


Fig: 4. specimen dimensions



Fig: 5. Tensile Test specimen

## RESULT AND DISCUSSION

### Hardness Test

The hardness test results are tabulated below, and these values are contrasted with those of several composites made of base Al 2011 alloy.

Table 1. Hardness values of AlTiB<sub>2</sub> composites

VHMN (cold rolled)					VMHN (hot rolled)
SAMPLE	TRAIL 1	TRAIL 2	TRAIL 3	AVG	AVG
0% AlTiB <sub>2</sub>	62	61	60	61	60.5
2% AlTiB <sub>2</sub>	65	67	65	65.6	62.4
4% AlTiB <sub>2</sub>	69	69	70	69.3	64
5% AlTiB <sub>2</sub>	74	72	74	73.3	67.66
6% AlTiB <sub>2</sub>	75	74	75	74.6	69.43
8% AlTiB <sub>2</sub>	77	80	75	77.3	73
10% AlTiB <sub>2</sub>	80	78	84	80.6	74.6

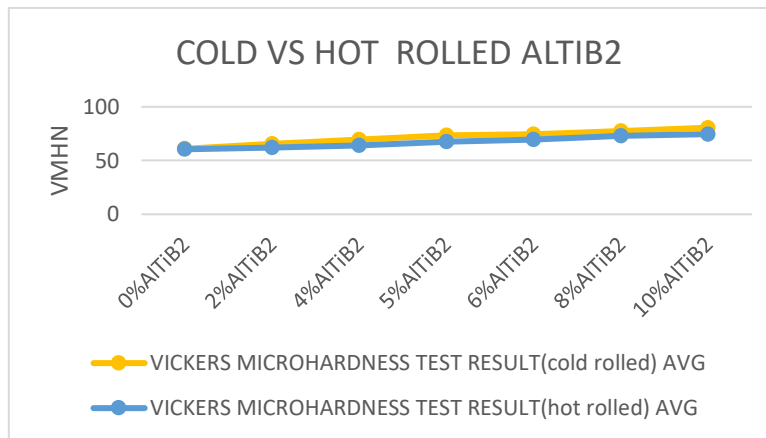


Fig: 6. Hardness test of AlTiB<sub>2</sub> composites graph

The hardness curves for various AlTiB<sub>2</sub> compositions that undergo hot rolling are displayed in Figure 6, and Table 1 has the relevant values. 8% AlTiB<sub>2</sub> yields a greater hardness number as a consequence than Al 2011. After hot rolling, the composite's hardness rises as the percentage of TiB<sub>2</sub> increases from HV 64 to 76.3, demonstrating that the addition of halide salts enhances the specimen's hardness. A matching graph is produced, displaying a comparative rise in hardness values between hot and cold rolled samples of the same proportions of TiB<sub>2</sub>. The hardness values of the cold and hot rolled samples were also listed in Table 1.[19]

## SEM CHARACTERIZATION

The subsequent figure displays the distinct microstructure composition of AlTiB<sub>2</sub>.

### 750X SEM

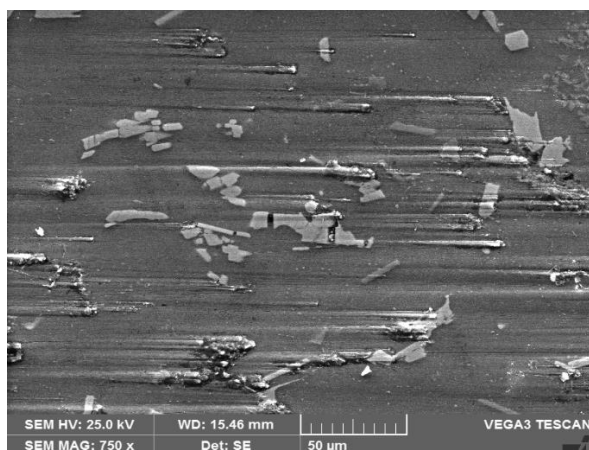


Fig: 7

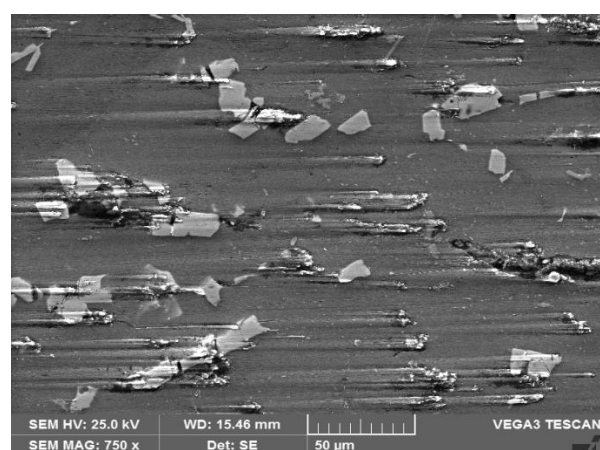


Fig: 8





Received: 16-01-2024

Revised: 12-02-2024

Accepted: 07-03-2024

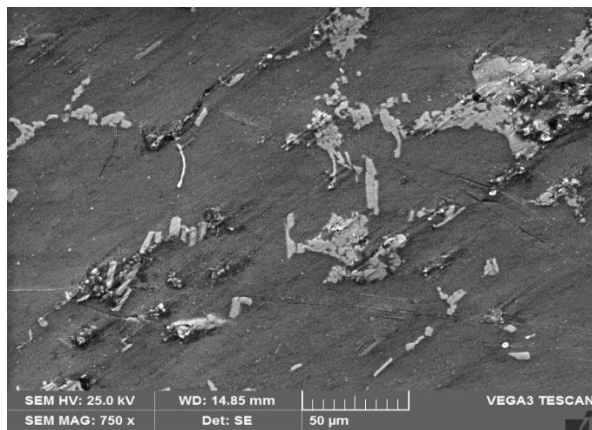


Fig: 9

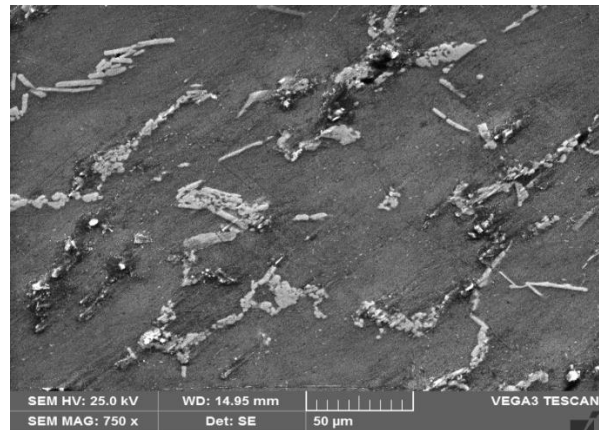


Fig: 10

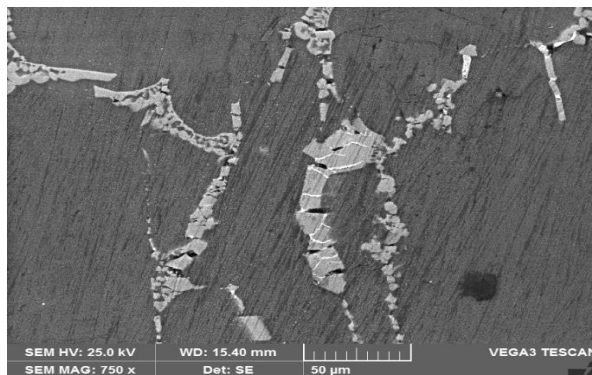


Fig: 11

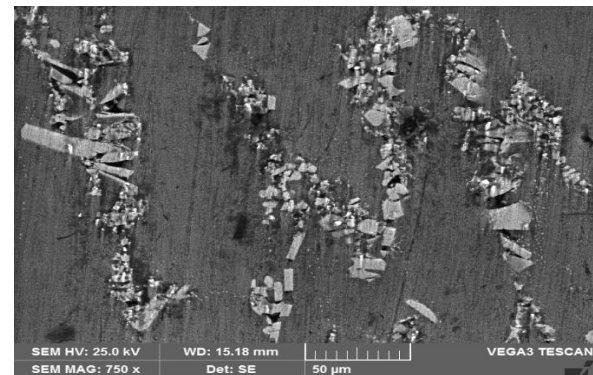


Fig: 12

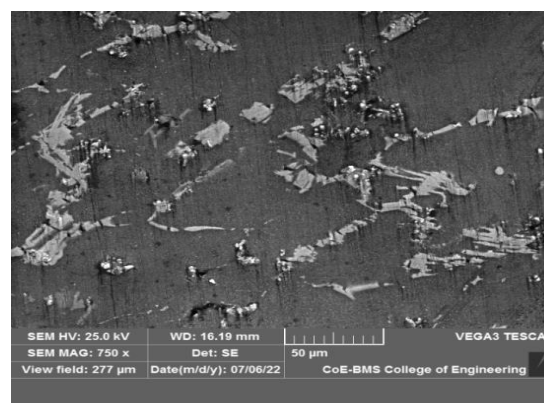


Fig:13

Figures 7 to 13 display the AlTiB<sub>2</sub> composite SEM images at 750X magnification, with proportions of 0,2,4,5,6,8 and 10%, respectively.



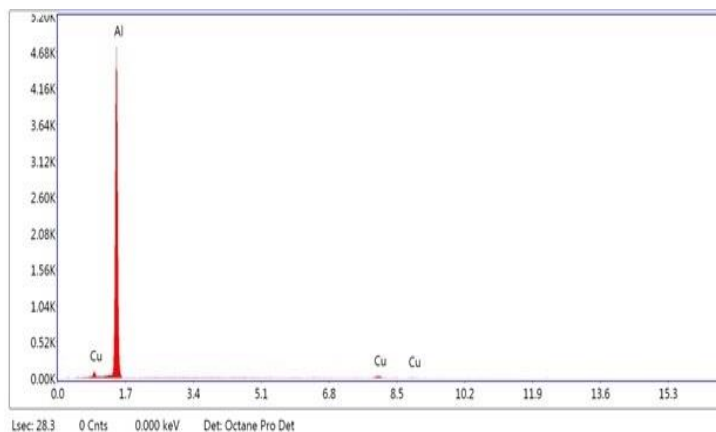


Fig. (7 to 13) displays the scanning electron microscopic pictures of the Al 2011 alloy with 0,2,4,5,6,8 and 10%  $\text{TiB}_2$  composites under cold rolled conditions, respectively, at a magnification of 750X as seen by the above figures, which shows the reinforcing particle, or white spots, at the grain boundaries. The distribution of tiny particles, aggregation, wetting characteristics, and any evident contaminants can all be seen in the SEM pictures. A rise in the fraction of added particles, or  $\text{TiB}_2$ , in the samples is observed to be the cause of the clusters in above SEM images that were identified as  $\text{TiB}_2$  and positioned near grain boundaries.

The microstructure observations show that the reinforcement particles are distributed rather evenly throughout the matrix and have a nearly spherical shape.  $\text{TiB}_2$  particles are characterized by the white spots, while porosity is revealed by the black spots. When the fraction of  $\text{TiB}_2$  in the composite grows during casting, white spots appear in the image, suggesting that particle clustering may be the result of insufficient stirring time and speed.

## EDAX Results

Table 2. EDAX Result OF 0%  $\text{TiB}_2$



Element	Weight %	Atomic %
Al K	95.67	98.01
Cu K	4.23	1.79

Fig 14. EDAX spectra graph of 0%  $\text{TiB}_2$ .

Table 3. EDAX Result OF 2%  $\text{TiB}_2$

Element	Weight %	Atomic %
B K	2.70	5.41
Al K	92.94	92.81
Ti K	0.30	0.16



Received: 16-01-2024

Revised: 12-02-2024

Accepted: 07-03-2024

Cu K	4.06	1.62
------	------	------

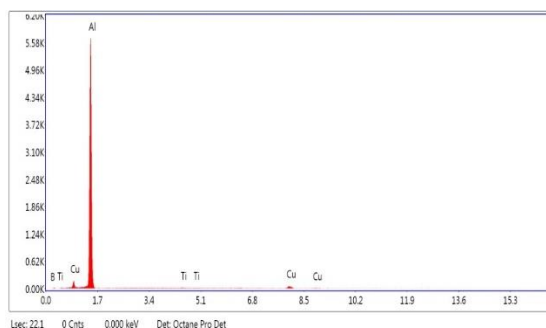
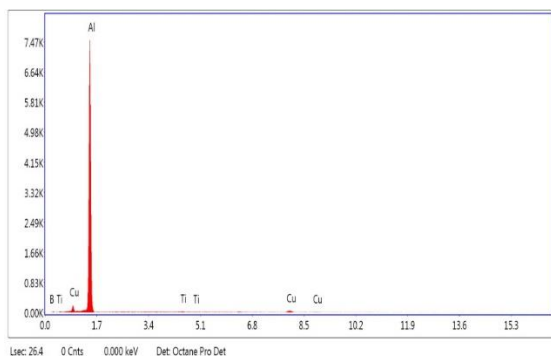


Fig 15. EDAX spectra graph of 2% TiB<sub>2</sub>.

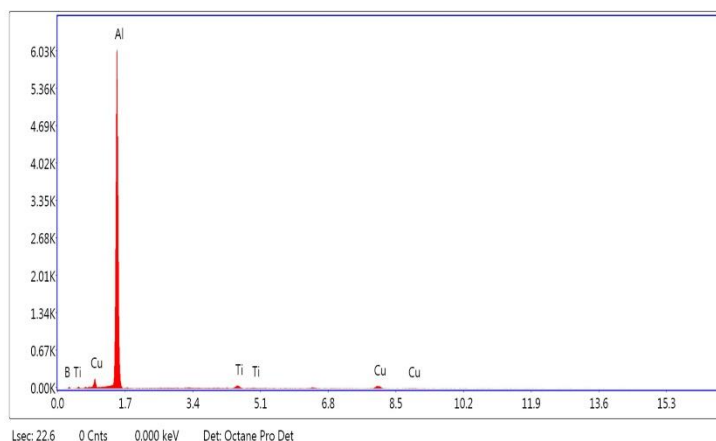
Table 4. EDAX Result OF 4% TiB<sub>2</sub>



Element	Weight %	Atomic %
B K	5.04	12.06
Al K	88.86	85.20
Ti K	1.93	1.04
Cu K	4.17	1.70

Fig 16. EDAX spectra graph of 4% TiB<sub>2</sub>.

Table 5. EDAX Result OF 5% TiB<sub>2</sub>

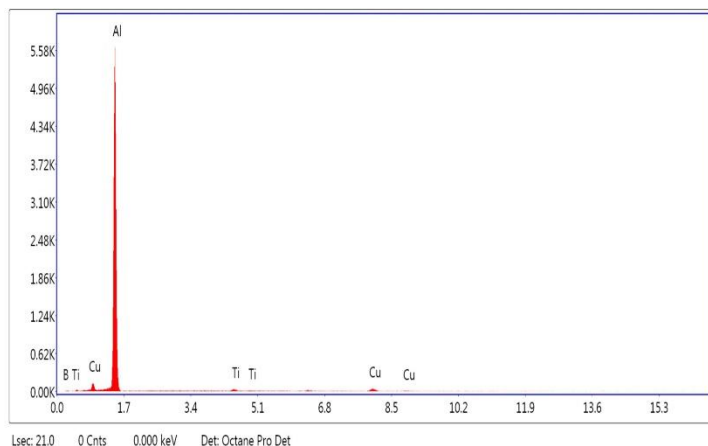


Element	Weight %	Atomic %
B K	6.12	14.41
Al K	88.36	83.33
Ti K	0.33	0.18
Cu K	5.19	2.08



Fig 17. EDAX spectra graph of 5% TiB<sub>2</sub>.

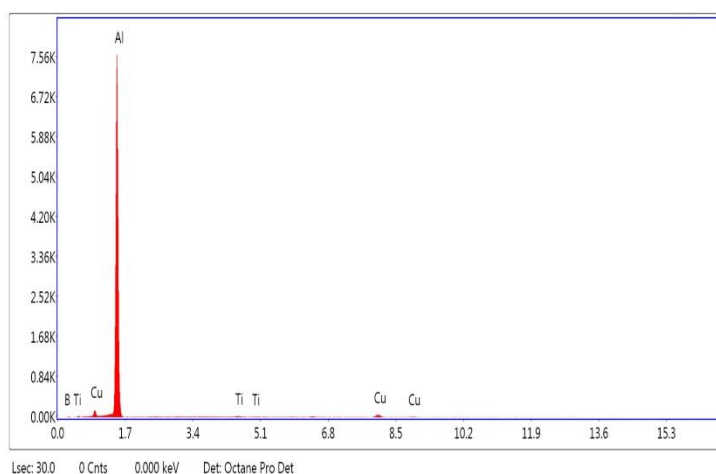
Table 6. EDAX Result OF 6% TiB<sub>2</sub>



Element	Weight %	Atomic %
B K	6.22	14.59
Al K	88.67	83.29
Ti K	0.63	0.33
Cu K	4.48	1.79

Fig 18. EDAX spectra graph of 6% TiB<sub>2</sub>.

Table 7. EDAX Result OF 8% TiB<sub>2</sub>



Element	Weight %	Atomic %
B K	7.64	17.47
Al K	88.22	80.86
Ti K	0.43	0.22
Cu K	3.71	1.44

Fig No. 19. EDAX spectra graph of 8% TiB<sub>2</sub>.

Table 8. EDAX Result OF 10% TiB<sub>2</sub>

Element	Weight %	Atomic %
B K	9.39	18.98
Al K	85.22	78.74
Ti K	1.35	0.70



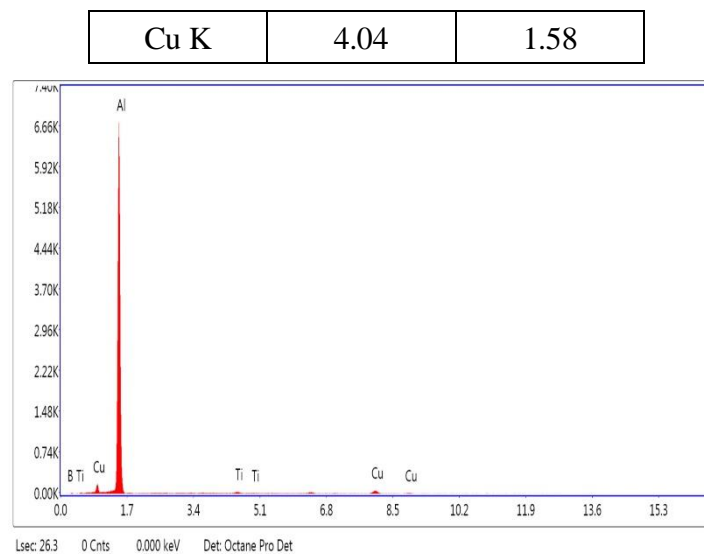


Fig 20. EDAX spectra graph of 10% TiB<sub>2</sub>.

## Discussion

TiB<sub>2</sub> occurs in the interfaces between Al2011, according to the EDAX pattern of the material under examination. The degree to which the matrix and reinforcement are bonded is significantly impacted by the existence of such brittle intermetallic phases. The experimental composites' EDAX patterns and material weight distribution (Al, Cu, B, and Ti) is shown in Figures (14 to 20) together with the tables that go with them. Aluminium is the predominant element, though, as the EDAX pattern demonstrates in all proportions.

## Corrosion Test

The corrosion test results are shown in the table below, and the corrosion rate was examined using the graph.

### Without Rolling:

Table 9. Corrosion Test Table Without Rolling

% of AlTiB <sub>2</sub> Composites	Ba (mV)	Bc (mV)	I Corr (mA/cm <sup>2</sup> )	Corrosion Rate (mm/year)	Corrosion rate (mils/yr.)
0	80.254	314.92	4.5154	64.224	2528.504
2	80.254	314.92	5.8975	49.173	1935.945
4	80.254	314.92	0.8827	47.107	1854.606



Received: 16-01-2024

Revised: 12-02-2024

Accepted: 07-03-2024

<b>5</b>	80.254	314.92	0.8827	46.532	1831.968
<b>6</b>	80.254	314.92	4.1337	45.016	1772.283
<b>8</b>	80.254	314.92	3.8865	42.096	1657.322
<b>10</b>	80.254	314.92	4.4111	40.932	1611.496

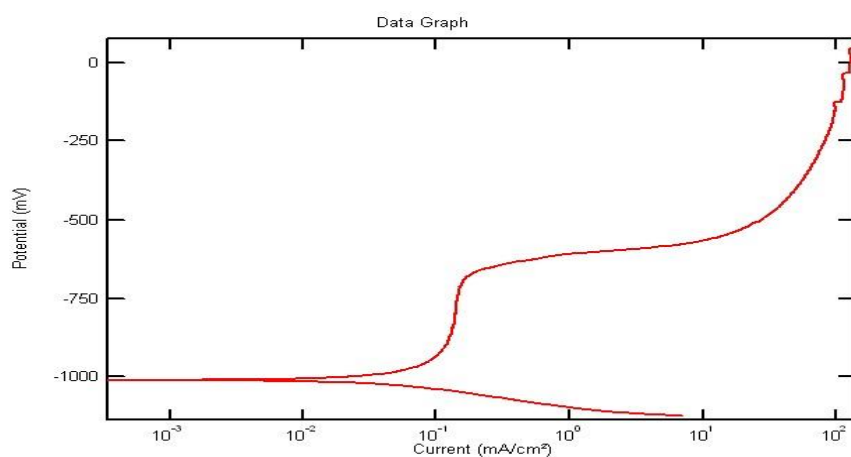


Fig: 21. 0% AlTiB<sub>2</sub> potentiodynamic scanning curves

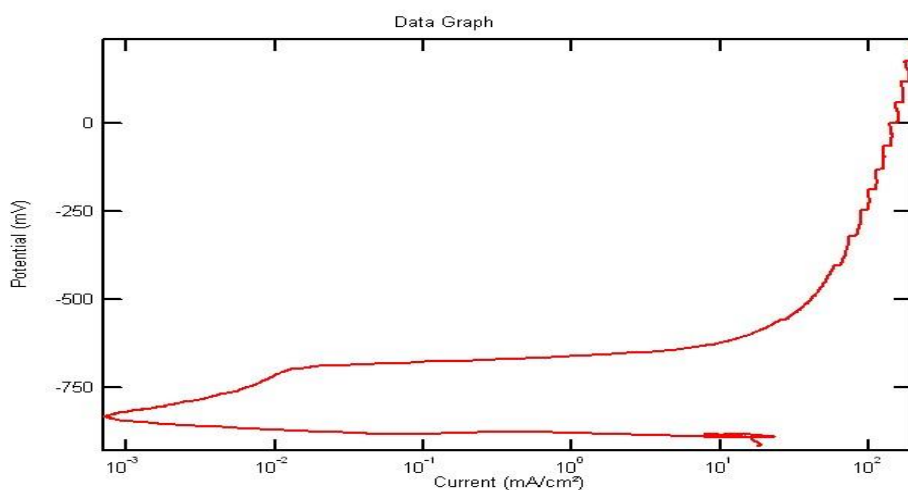


Fig: 22. 2% AlTiB<sub>2</sub> potentiodynamic scanning curves



Received: 16-01-2024

Revised: 12-02-2024

Accepted: 07-03-2024

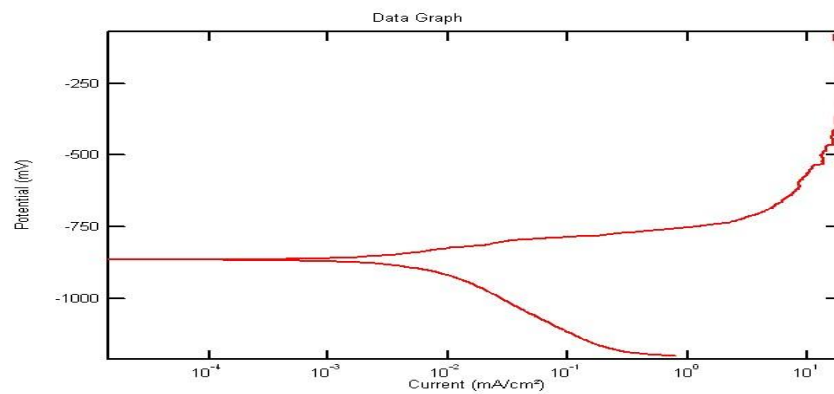


Fig. 23. 4% AlTiB<sub>2</sub> potentiodynamic scanning curves

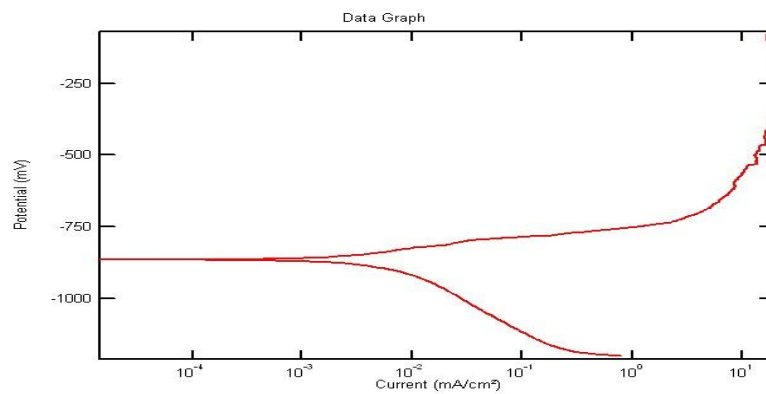


Fig. 24. 5% AlTiB<sub>2</sub> potentiodynamic scanning curves

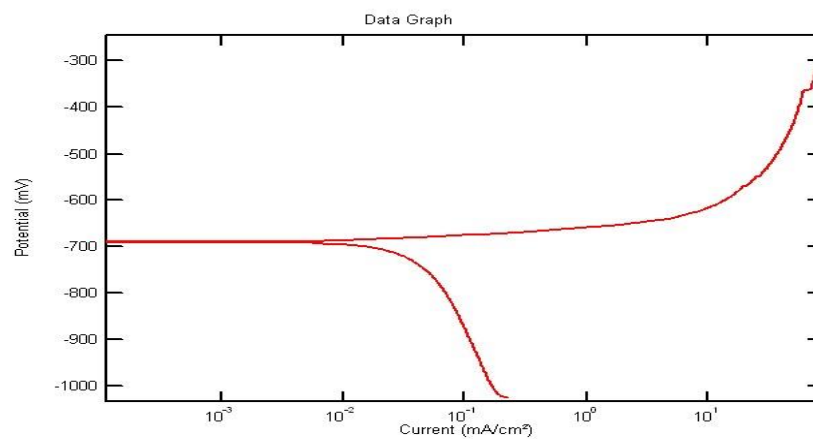


Fig. 25. 6% AlTiB<sub>2</sub> potentiodynamic scanning curves



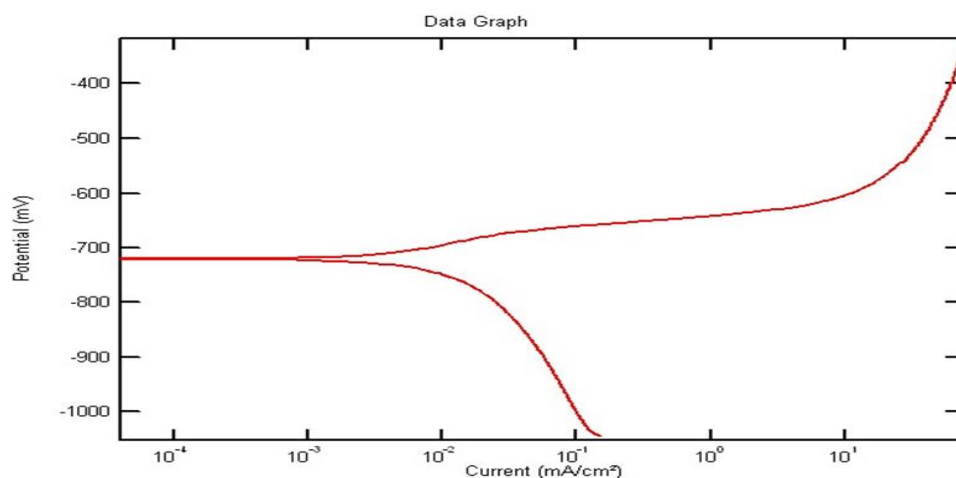


Fig: 26. 8% AlTiB<sub>2</sub> potentiodynamic scanning curves

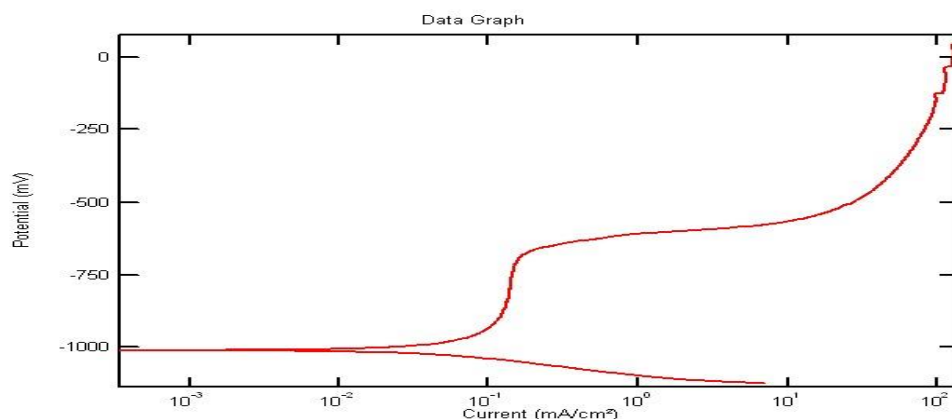


Fig: 27. 10% AlTiB<sub>2</sub> potentiodynamic scanning curves

### With Rolling

Table 10. Corrosion Test Table with Rolling

% of AlTiB <sub>2</sub> Composites	Ba (mV)	Bc (mV)	I Corr (mA/cm <sup>2</sup> )	Corrosion Rate (mm/year)	Corrosion rate (mils/yr.)
0	80.254	314.92	2.9155	31.75	1250
2	80.254	314.92	2.9722	32.368	1274.3



Received: 16-01-2024

Revised: 12-02-2024

Accepted: 07-03-2024

4	80.254	314.92	2.9155	33.276	1293.1
5	80.254	314.92	2.9155	34.504	1299.5
6	80.254	314.92	2.9155	35.113	1305.3
8	80.254	314.92	2.9155	36.981	1345.1
10	80.254	314.92	2.9155	37.532	1367.8

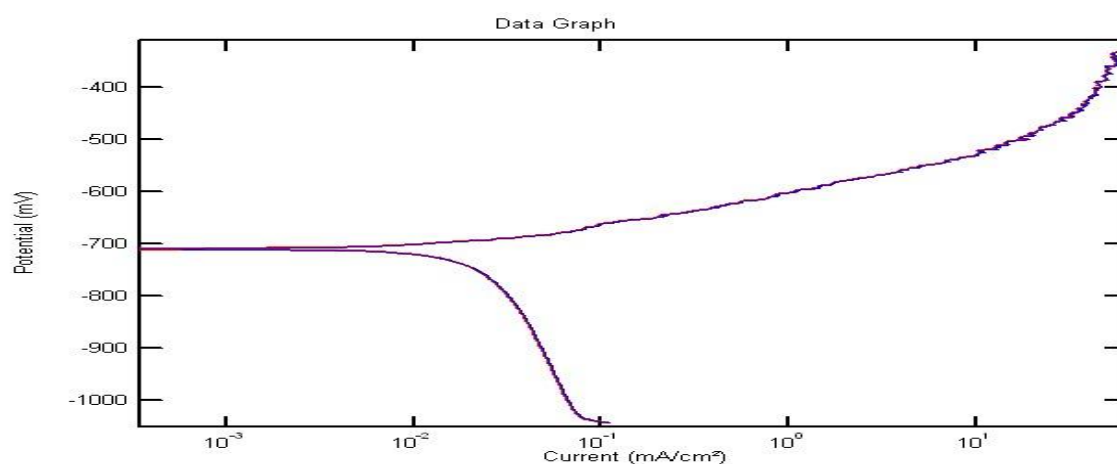


Fig: 28. 0% AlTiB<sub>2</sub> potentiodynamic scanning curves

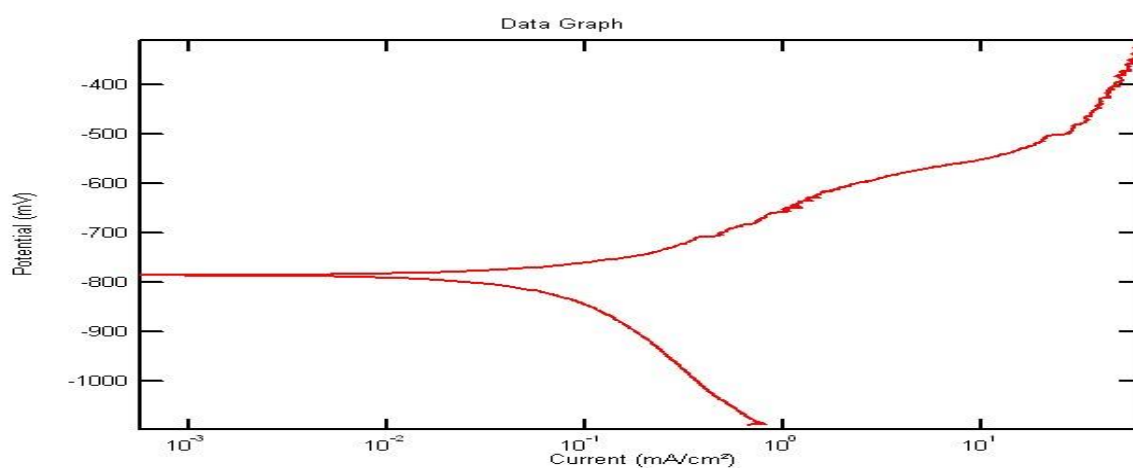


Fig: 29. 2% AlTiB<sub>2</sub> potentiodynamic scanning curves



Received: 16-01-2024

Revised: 12-02-2024

Accepted: 07-03-2024

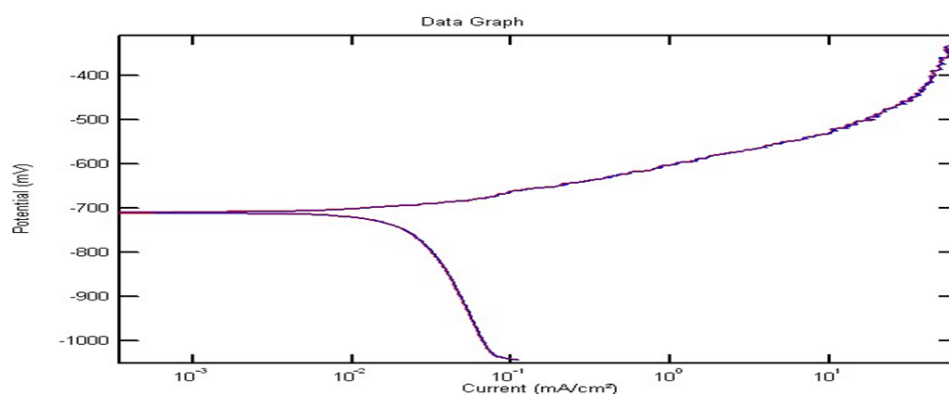


Fig: 30. 4% AlTiB<sub>2</sub> potentiodynamic scanning curves

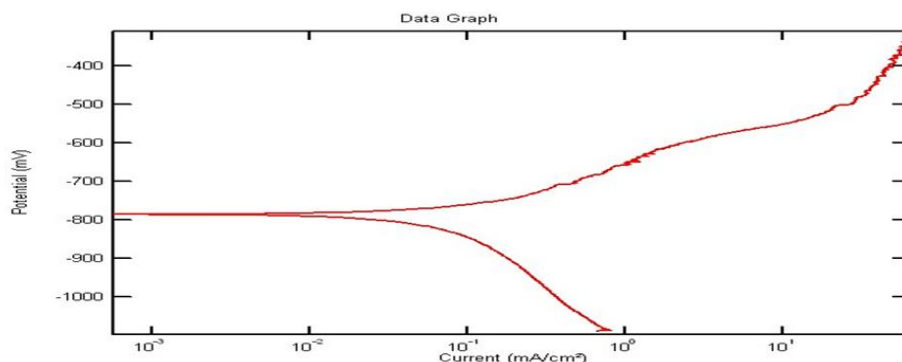


Fig: 31. 6% AlTiB<sub>2</sub> potentiodynamic scanning curves

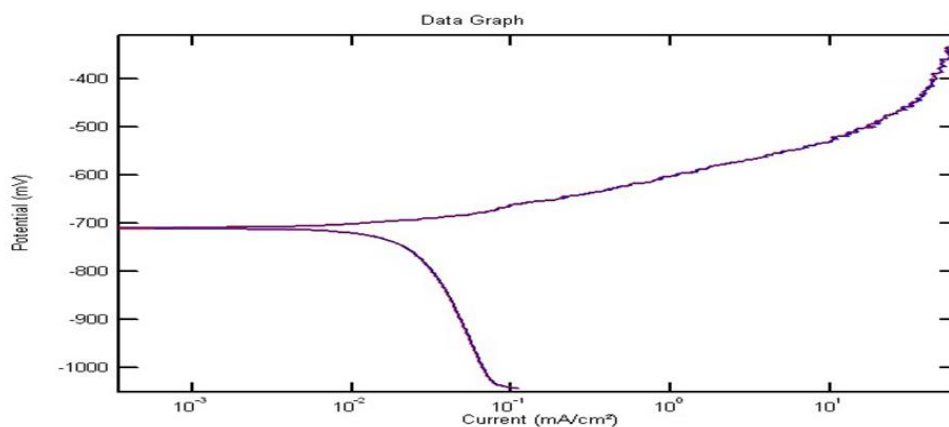


Fig: 32. 8% AlTiB<sub>2</sub> potentiodynamic scanning curves





Received: 16-01-2024

Revised: 12-02-2024

Accepted: 07-03-2024

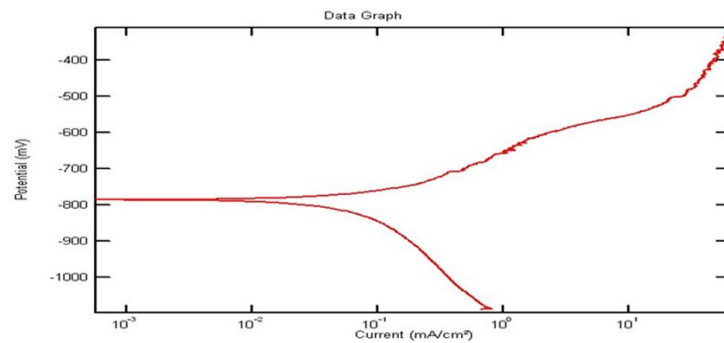


Fig: 33. 10% AlTiB<sub>2</sub> potentiodynamic scanning curves

Table 11. Comparison of Corrosion rate of with and Without Hot rolling of AlTiB<sub>2</sub>

SL No	% of AlTiB <sub>2</sub> composites	Corrosion rate Without Hot Rolling of AlTiB <sub>2</sub>	Corrosion rate Hot Rolling of AlTiB <sub>2</sub>
1	0	64.244	31.750
2	2	49.173	32.368
3	4	47.101	33.276
4	5	46.532	34.356
5	6	45.016	35.113
6	8	42.096	36.981
7	10	40.932	37.532

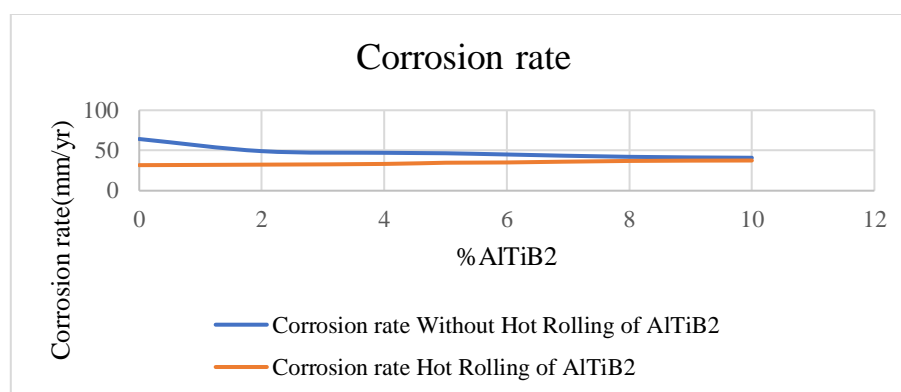


Fig.34. Corrosion rate of AlTiB<sub>2</sub>



## Discussion:

It is evident from Figure 34. that the corrosion resistance of the composites has improved following the hot rolling treatment. These figures compare the corrosion rate of AlTiB<sub>2</sub> with and without hot rolling.

Following hot rolling, the corrosion behaviour of AlTiB<sub>2</sub> composites was investigated at room temperature in a 3.5 weight percent NaCl solution. The results showed that the corrosion of the composites began at the interfaces between the TiB<sub>2</sub> particles and the Al matrix. During the hot rolling deformation, the particle distribution in the composites has become more uniform.

Comparing the as-cast AlTiB<sub>2</sub> composites to the rolling process, the results demonstrated a considerable improvement in corrosion resistance in a 3.5 weight percent NaCl solution. Furthermore, the rolled specimen containing 0 percent AlTiB<sub>2</sub> exhibited the highest level of corrosion resistance in the composites. This was attributed to a superior passive film on the surface resulting from enhanced matrix and particle bonding with decreased porosity and consistent reinforcement particle distribution [17].

## TENSILE TEST

The tensile test results are tabulated below, and base Al 2011 and cold-rolled AlTiB<sub>2</sub> composites are contrasted with these values.

### Comparison Study with Hot Rolled and Cold Rolled of Tensile Test

TENSILE TEST RESULTS (COLD ROLLED)				TENSILE TEST RESULTS (HOT ROLLED)		
SAMPL E	UTS (Mpa)	YS (Mpa)	% ELONGATI ON	UTS (Mpa)	YS (Mpa)	% ELONGATI ON
0%AlTiB <sub>2</sub>	200	160	18	238	196.6	20.6
2%AlTiB <sub>2</sub>	220	174	15.5	235	195.2	20.2
4%AlTiB <sub>2</sub>	238	182	13.1	228	192	19.9
5%AlTiB <sub>2</sub>	244	189	12.2	221	193	19.6



6%AlTiB <sub>2</sub>	260	192	11.5	218	171	17.2
8%AlTiB <sub>2</sub>	278	220	11.1	200	162	10.5
10%AlTiB <sub>2</sub>	290	235	10.8	177	156.1	4.5

Table 8. Tensile test results (Hot and cold rolled)

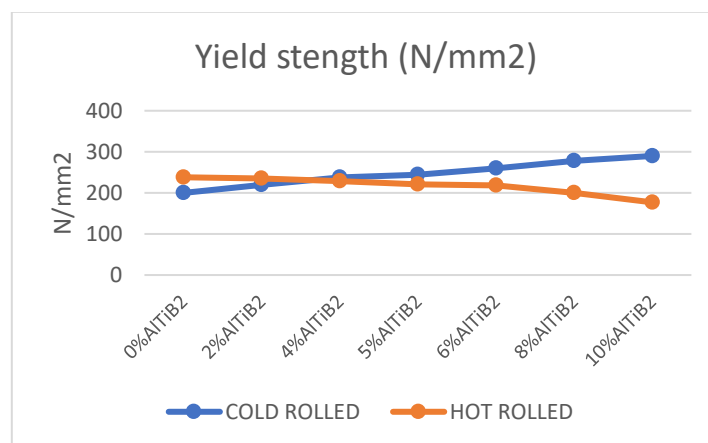


Fig.30. shows the graph of UTS vs different proportions of TiB<sub>2</sub> for hot and cold rolled specimens

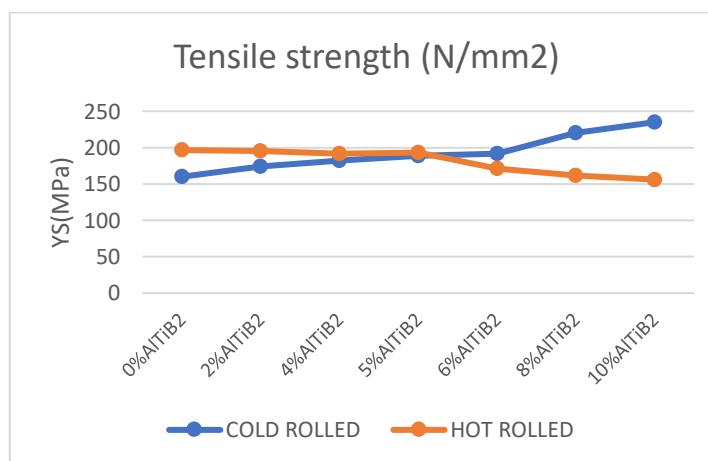


Fig.31. shows the variation of yield strength vs different proportions of TiB<sub>2</sub> for hot and cold rolled specimens



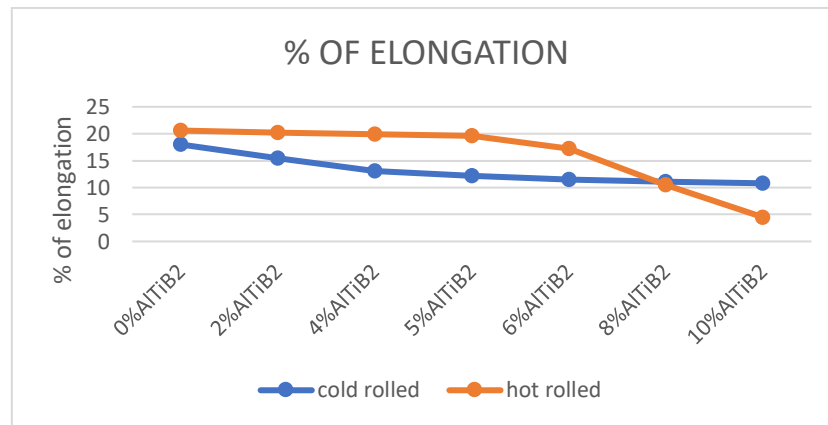


Fig.32. shows the graph of % of elongation vs different proportions of  $TiB_2$  for hot and cold rolled specimens

Figures 30, 31, and 32 display the appropriate graphs and table 8 contains the results of the tensile properties of  $AlTiB_2$  with varying compositions after cold and hot rolling. A drop in the tensile strength of 238 to 177 MPa has been found in hot rolled samples. In addition, the yield strength of the  $AlTiB_2$  composite decreases from 196 to 156 MPa, and the percentage of elongation decreases in proportion to the rise in  $TiB_2$  concentration. Increases in cold rolled sample tensile values confirm the high density of particle dislocations. In [18].

## CONCLUSION

$AlTiB_2$  composites were made using the stir casting process and the in-situ approach, with varying weight percentages (0, 2, 4, 5, 6, 8, 10%) of  $TiB_2$ . The existence and reasonably good dispersion of  $TiB_2$  particles in the Al matrix are demonstrated by the SEM and EDAX data. Furthermore, following cold rolling, it is seen in SEM that the grains lengthened along the rolling direction. The distribution of the grains in  $AlTiB_2$  composite is significantly impacted by rolling, particularly at lower and higher rolling temperatures, which can have an impact on the mechanical properties. Hot rolled composites reinforced with 4, 6 and 8%  $TiB_2$  show a higher Vickers micro hardness value than hot rolled Al 2011 (i.e.,  $Al_{2011} + 0\% TiB_2$ ). Vickers micro hardness values of cold rolled samples are relatively high as compared to hot rolled samples that have the same weight percentage of  $TiB_2$ . Titanium Di Boride content in Al composites plays a major function in the object's protective layer. The strength of the base material will cause an increase in the proportion of  $TiB_2$  addition with Al 2011. When comparing the wear rates of the three composites, it becomes less as the amount of  $TiB_2$  increases. As the percentage of  $TiB_2$  grows, the composite's hardness value correspondingly



risers. This results in a more uniform dispersion of the reinforced phase, as the previously stated microstructure amply illustrates. It is clear from comparing the outcomes of cold- and hot-rolled samples that the tensile and yield strengths of the cold-rolled samples rise with an increase in  $\text{TiB}_2$  content. The significant density of dislocations in the cold-rolled sample provided justification for these findings. However, the yield strength and % of elongation rapidly falls in hot rolling due to the heat treatment applied before to the rolling operation.

## REFERENCES

- [1] Veeravalli Rama Koteswara Roa etc, Dept. Of Mechanical Engineering Guntur 522019 India, Mechanical and Tribological Properties of AA7075-TIC MMC Under Heat Treated and Cast Conditions.
- [2] Preetam Kulkarni, Dept of Mechanical Engineering, University Visvesvaraya college of Engineering India, Evaluation of Mechanical Properties of AL2024 Based Metal Composites.
- [3] S. Suresh, Dept. Of Mechanical Engineering and university of Technology Tirunevali, Tamil Nadu. N. Shenbaga vinayaga moorthi, Dept of Mechanical Engg and university of Technology, Tirunevali, Tamil Nadu.
- [4] M.M. SIVA, R. RAJESH, S. PUGAZHENDHI & M. SIVAPRAGASH Research Scholar, Mechanical Engineering Department, Noorul Islam University, Kumaracoil, Tamil Nadu, India
- [5]. Dolata AJ, Jakub W (2007) Tribological properties of hybrid composites containing two carbide phases
- [6] Vignesh.V.Shanbagh, Nitin.N.Yalamoori, S. Karthikeyan, R. Ramanujam.R and K. Venkatesan, "Fabrication, Surface Morphology and corrosion investigation of Al7075-Al<sub>2</sub>O<sub>3</sub> matrix composite in sea water and Industrial environment", Procedia Engineering (GCM 2014), No. 97, pp. 607-613, 2014.
- [7] MAHENDRA KV AND K. RADHAKRISHNA (2010) Characterization of Stir Cast Al Cu (fly ash + SiC) Hybrid Metal Matrix Composites. 44:
- [8]. Lee MH, Kim JH, Park JS et al (2004) Fabrication of Ni-Nb-Ta metallic glass reinforced Al-based alloy matrix composites by infiltration casting process. ScrMater50:1367–1371
- [9]. Boopathi M, Arulshri KP, Iyandurai N (2013) Evaluation of Mechanical Properties of Aluminium Alloy2024 Reinforced with Silicon Carbide and Fly Ash Hybrid Metal Matrix Composites. 10:219– 229.
- [10] S. Rajesha.S, C.S. Jawalkar, Radha Raman Mishra, A.K. Sharma and Pradeep Kumar, "Study of recast layers of surface roughness on Al-7075 metal matrix composite during EDM machining", International Journal of Recent advances in Mechanical Engineering, Vol. 3, No. 1, pp. 53-62, 2014.



- [11]. Mohan Kumar S, Pramod R, Shashi Kumar M E, Govindaraju H K “Evaluation of Fracture Toughness and Mechanical Properties of Aluminium Alloy 7075, T6 with Nickel Coating” ScienceDirect, Procedia Engineering 97 (2014) 178 – 185
- [12] Gupta, M., Mohamed, F., Lavernia, E., & Srivatsan, T. S. (1993). Microstructural evolution and mechanical properties of SiC/Al<sub>2</sub>O<sub>3</sub> particulate- reinforced spray-deposited metal-matrix composites. Journal of materials science, 28(8), 2245-2259.
- [13] Lloyd, D. J. (1994). Particle reinforced aluminium and magnesium matrix composites. International Materials Reviews, 39(1), 1-23.
- [14] Ibrahim, I. A., Mohamed, F. A., & Lavernia, E. J. (1991). Particulate reinforced metal matrix composites—a review. Journal of materials science, 26(5), 1137-1156.
- [16] H.S. Dr. Manjunatha et al 2021 Wear Behaviour of Aluminium-TiB<sub>2</sub> Metal Matrix Composites. Assistant Professor, Department of Mechanical Engineering, ATMECE, Mysore, Karnataka, India, IOP Conf. Ser.: Mater. Sci. Eng. 1189 012007
- [17] Nie, J., Wang, F., Chen, Y., Mao, Q., Yang, H., Song, Z, Zhao, Y. (2019). Microstructure and corrosion behavior of Al-TiB<sub>2</sub>/TiC composites processed by hot rolling. Results in Physics,14,102471. Doi: 10.1016/j.rinp.2019.102471
- [18] M. Tajally , Z. Huda and H.H. Masjuki , Effect of cold rolling on bending and tensile behaviour of 7075 Al alloy ,Journal of Applied Sciences (2009)
- [19] Bo WANG, Xian-hua CHEN, Fu-sheng PAN, Jian-jun MAO1, Yong FANG, Effects of cold rolling and heat treatment on microstructure and mechanical properties of AA 5052 aluminium alloy. Article in Transactions of Nonferrous Metals Society of China · August 2015 DOI: 10.1016/S1003-6326(15)63866-3